General Procedures

All reactions were performed under argon atmosphere unless otherwise noted. A glovebox of the type UniLab/MBraun (Ar 4.8, O_2 < 1 ppm, H_2O < 1 ppm) was used for storage and weighing of sensitive compounds. All analytical samples that required the absence of oxygen were prepared in the same glovebox. Dichloromethane was dried with CaH_2 and distilled prior to use. THF was distilled from potassium. All reagents were used as received from commercial suppliers (ABCR, Acros Organics, Alfa Aesar, Fischer Scientific, Fluka and Sigma-Aldrich). Deuterated solvents were purchased from euriso-top. $W(CO)_5[C(Fc)OEt]$ was synthesized using literature procedures.[1] NMR spectra were recorded on a Bruker Avance DRX 400 spectrometer at 400.31 MHz (^1H) and 100.07 MHz ($^{13}C\{^1H\}$). All resonances are reported in ppm versus the solvent signal as internal standard [CD_3CN (^1H: $\delta = 1.94$), CD_2Cl_2 (^1H: $\delta = 5.32$ ppm; ^{13}C: $\delta = 54.0$ ppm)].[2] IR spectra were recorded as solid state samples with a Bruker ALPHA II FT-IR spectrometer with a platinum Di-ATR module. Electrochemical experiments were carried out on a BioLogic SP-50 voltammetric analyser using platinum wires as counter and working electrodes and a 0.01 M $Ag/AgNO_3$ electrode as reference electrode. The cyclic voltammetry measurements were carried out at scan rate of 50–100 mV s^{-1} using 0.1 M $[n\text{Bu}_4\text{N}][\text{B}(\text{C}_6\text{F}_5)_4]$ or 0.1 M $[n\text{Bu}_4\text{N}][\text{PF}_6]$ as supporting electrolytes in CH_2Cl_2 of THF. Potentials are referenced to the ferrocene/ferrocenium couple ($E_{½}$ = 220 ± 5 mV under the experimental conditions). UV/Vis/NIR spectra were recorded on a Varian Cary 5000 spectrometer using 1.0 cm cells (Hellma, suprasil). FD mass spectra were recorded on a Thermo Fisher DFS mass spectrometer with a LIFDI upgrade. Elemental analyses were performed by the microanalytical laboratory of the chemical institutes of the University of Mainz. ^{57}Fe Mößbauer measurements of powder samples were performed in transmission geometry using a constant-acceleration spectrometer and the source ^{57}Co(Rh). The Recoil 1.03 Mössbauer Analysis Software was used to fit the experimental spectra with Lorentzian peaks.[3] Isomer shift values are quoted relative to α-Fe at 293 K. X-band CW EPR spectra were measured on a Miniscope MS 300 at 77 K cooled by liquid nitrogen in a finger Dewar and at 298 K (Magnettech GmbH, Berlin, Germany). *g* factors are referenced to external Mn^{2+} in ZnS (g = 2.118, 2.066, 2.027, 1.986, 1.946, 1.906). Simulations of EPR spectra were performed with EasySpin (v 5.0.0) for MatLab (R2016b).[4] XAS spectral measurements were performed at beamline P64 of PETRA III (Hamburg, Germany) under ambient conditions at 293 K. A Si(111) double crystal monochromator was used for measurements at the Au L_3-edge (11.918 keV). The second monochromator crystal was tilt for optimal harmonic rejection. Energy calibration was performed with a gold metal foil. The samples were handled in a glove box. All samples were prepared as self supporting wafers using degassed BN as binder.

DFT calculations

Density functional theory calculations were carried out using the ORCA program package (version 4.0.1).[5] All calculations were performed using the B3LYP functional[6–8] and employ the RIJCOSX approximation.[9,10] Relativistic effects were calculated at the zeroth order regular approximation (ZORA) level.[11] The ZORA keyword automatically invokes relativistically adjusted basis sets. To account for solvent effects, a conductor-like screening model (CPCM) modelling dichloromethane was used in all calculations.[12,13] Geometry optimizations were performed using Ahlrichs' split-valence triple-ξ basis set ZORA-def2-TZVP.[14] The auxiliary basis set for General-purpose Coulomb fitting SARC/J decontracted def2/J up to Kr was used.[15] The segmented all-electron relativistically contracted (SARC) auxiliary basis set beyond Kr, SARC-ZORA-TZVP, was used for gold and a special grid of 7 (default 4).[11,16–19] Atom-pairwise dispersion correction was performed with the Becke-Johnson damping scheme (D3BJ).[20,21] The presence of energy minima was checked by numerical frequency calculations.

Synthesis of 1, AuCl[C(Fc)OEt]

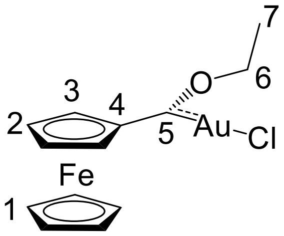

A slightly modified literature procedure for the synthesis of AuCl[C(Fc)OMe] was used for the synthesis of **1**.[22] To a solution of W(CO)$_5$[C(Fc)(OEt)][23] (1 mmol, 565.5 mg, 1 eq) in THF (10 mL) chlorido(dimethylsulfide)gold(I) (1 mmol, 294.6 mg, 1 eq) was added under stirring at 0 °C. The deep red solution was stirred at this temperature for 6 h. After filtration, *n*-heptane (10 mL) was added and the red-purple solution was stored at –28 °C for 3 days. Filtration yielded a deep purple solid. Yield 340.4 mg (0.72 mmol 72 %). ^{1}H NMR (400.32 MHz, CD$_2$Cl$_2$): δ = 5.17 (pt, 2H, H^2), 5.00 (q, $^3J_{HH}$ = 8 Hz, 2H, H^6), 5.00 (pt, 2H, H^3; under the q of the OCH$_2$ group confirmed by COSY), 4.47 (s, 5H, H^1), 1.56 (t, $^3J_{HH}$ = 8 Hz, 3H, H^7) ppm. ^{1}H NMR (400.32 MHz, CD$_3$CN) δ = 5.25 (pt, 2H, H^2), 5.03 (pt, 2H, H^3), 4.96 (q, $^3J_{HH}$ = 8 Hz, 2H, H^6), 4.50 (s, 5H, H^1), 1.54 (t, $^3J_{HH}$ = 8 Hz, 3H, H^7) ppm. ^{13}C NMR (100.07 MHz, CD$_2$Cl$_2$): δ = 250.9 (C^5), 87.2 (C^4), 80.3 (C^3), 79.5 (C^2), 79.0 (C^6; confirmed by HSQC), 72.1 (C^1), 15.3 (C^7) ppm. MS (FD): *m/z* (%) = 474.3 (100) [M]$^+$. IR (ATR) $\tilde{\nu}$ = 3092 (w), 2933 (w), 1364 (m) 1107 (m), 826 (m), 823 (m), 480 (s) cm^{-1}. UV/Vis (CH$_2$Cl$_2$): λ_{max} (ε) = 266 (2270), 304 (3550), 374 (1010), 521 (1040 M^{-1} cm^{-1}) nm. Anal. Calcd for C$_{13}$H$_{14}$FeAuClO (473.97): C, 32.90; H, 2.97. Found: C, 32.60; H 2.87.

General Procedure for the Catalytic Cyclization of *N*(2-propyn-1-yl)benzamide to 2-phenyl-5-vinylidene-2-oxazoline

N-Prop-2-yne-benzamide (15.9 mg, 0.1 mmol, 1 eq) was dissolved in CD$_2$Cl$_2$ (1 mL) in an inert-gas NMR tube, **1** (0.5 mg, 1.0×10^{-3} mmol, 1 mol-%), tris(4-bromophenyl)ammoniumyl hexachloroantimonate (Magic Blue; 1.0 mg, 1.25×10^{-3} mmol, 1.25 mol %) and *n*-hexadecane (3 µL) as internal standard were added. ^{1}H NMR spectra were recorded over time. The proton resonances (*ortho* protons of phenyl ring, H^3) of the starting material (δ = 7.77) and the product (δ = 7.98) were integrated.

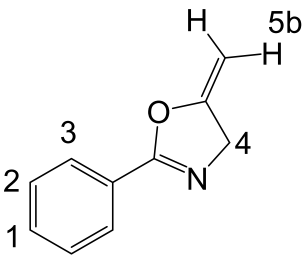

EPR calibration

Quantification of the EPR signals was performed via an adapted literature procedure.[24,25] For quantification measurements, EPR tubes with an internal diameter of 2.0 mm were used. The calibration curve was determined using commercially available tetraphenylporphyrinato copper(II) (CuTPP) as standard. The samples were prepared in a glovebox under argon, and the EPR tubes were filled with 400 µL of the solution and sealed with Critoseal. They were inserted 10.4 cm (measured at the Teflon holder) into the EPR spectrometer. Four concentrations (c = 1.67, 0.84, 0.42 and 0.21 mᴍ) in THF were used for the calibration. The settings for the calibration curve and the sample EPR spectra were as follows: temperature = 298 K, field = 3360 G, sweep = 800 G, sweep time = 300 s, modulation = 2000 mG, MW attenuation = 6 db, and number of passes = 3. The double integral of the experimental, baseline corrected spectra was plotted against the concentration. The resulting calibration (linear regression; $y = (2.97 \pm 0.03) \times 10^6 \times c(\text{mM})$; $R^2 = 0.9986$) was used to quantify the experimental spectra of **1** after oxidation with Magic Blue.

References

[1] J. G. López-Cortés, L. F. La Contreras de Cruz, M. C. Ortega-Alfaro, R. A. Toscano, C. Alvarez-Toledano and H. Rudler, *J. Org. Chem.*, 2005, **690**, 2229–2237.

[2] G. R. Fulmer, A. J. M. Miller, N. H. Sherden, H. E. Gottlieb, A. Nudelman, B. M. Stoltz, J. E. Bercaw and K. I. Goldberg, *Organometallics*, 2010, **29**, 2176–2179.

[3] K. Lagarec and D. G. Rancourt, *Nucl. Instrum. Methods Phys. Res. B*, 1997, **129**, 266–280.

[4] S. Stoll and A. Schweiger, *J. Magn. Reson.*, 2006, **178**, 42–55.

[5] F. Neese, *WIREs Comput Mol Sci* 2012, **2**, 73–78.

[6] A. D. Becke, *J. Chem. Phys.* 1993, **98**, 5648–5652.

[7] C. Lee, W. Yang and R. G. Parr, *Phys. Rev. B* 1988, **37**, 785–789.

[8] B. Miehlich, A. Savin, H. Stoll and H. Preuss, *Chem. Phys. Lett.* 1989, **157**, 200–206.

[9] F. Neese, F. Wennmohs, A. Hansen and U. Becker, *Chem. Phys.* 2009, **356**, 98–109.

[10] R. Izsák and F. Neese, *J. Chem. Phys.* 2011, **135**, 144105.

[11] D. A. Pantazis, X.-Y. Chen, C. R. Landis and F. Neese, *J. Chem. Theory Comput.*, 2008, **4**, 908–919.

[12] V. Barone and M. Cossi, *J. Phys. Chem. A*, 1998, **102**, 1995–2001.

[13] S. Miertuš, E. Scrocco and J. Tomasi, *Chem. Phys.*, 1981, **55**, 117–129.

[14] F. Weigend and R. Ahlrichs, *Phys. Chem. Chem. Phys.*, 2005, **7**, 3297–3305.

[15] F. Weigend, *Phys. Chem. Chem. Phys.*, 2006, **8**, 1057–1065.

[16] D. A. Pantazis and F. Neese, *J. Chem. Theory Comput.*, 2009, **5**, 2229–2238.

[17] D. A. Pantazis, X. Y. Chen, C. R. Landis and F. Neese, *J. Chem. Theory Comput.* 2008, **4**, 908–919.

[18] D. A. Pantazis and F. Neese, *Theor. Chem. Acc.*, 2012, **131**, 1292–1298.

[19] D. A. Pantazis and F. Neese, *J. Chem. Theory Comput.*, 2011, **7**, 677–684.

[20] S. Grimme, J. Antony, S. Ehrlich and H. Krieg, *J. Chem. Phys.* 2010, **132**, 154104.

[21] S. Grimme, S. Ehrlich and L. Goerigk, *J. Comput. Chem.* 2011, **32**, 1456–1465.

[22] D. I. Bezuidenhout, B. van der Westhuizen, A. J. Rosenthal, M. Wörle, D. C. Liles and I. Fernández, *Dalton Trans.*, 2014, **43**, 398-401.

[23] J. A. Connor and J. P. Lloyd, *Dalton Trans.*, 1972, 1470–1476.

[24] A. Neidlinger, T. Kienz and K. Heinze, *Organometallics*, 2015, **34**, 5310–5320.

[25] G. R. Eaton, S. S. Eaton, D. P. Barr and R. T. Weber, *Quantitative EPR*; Springer: Wien, NY, 2010.

Fig. S01. ^{1}H NMR spectrum of **1** in CD_2Cl_2.

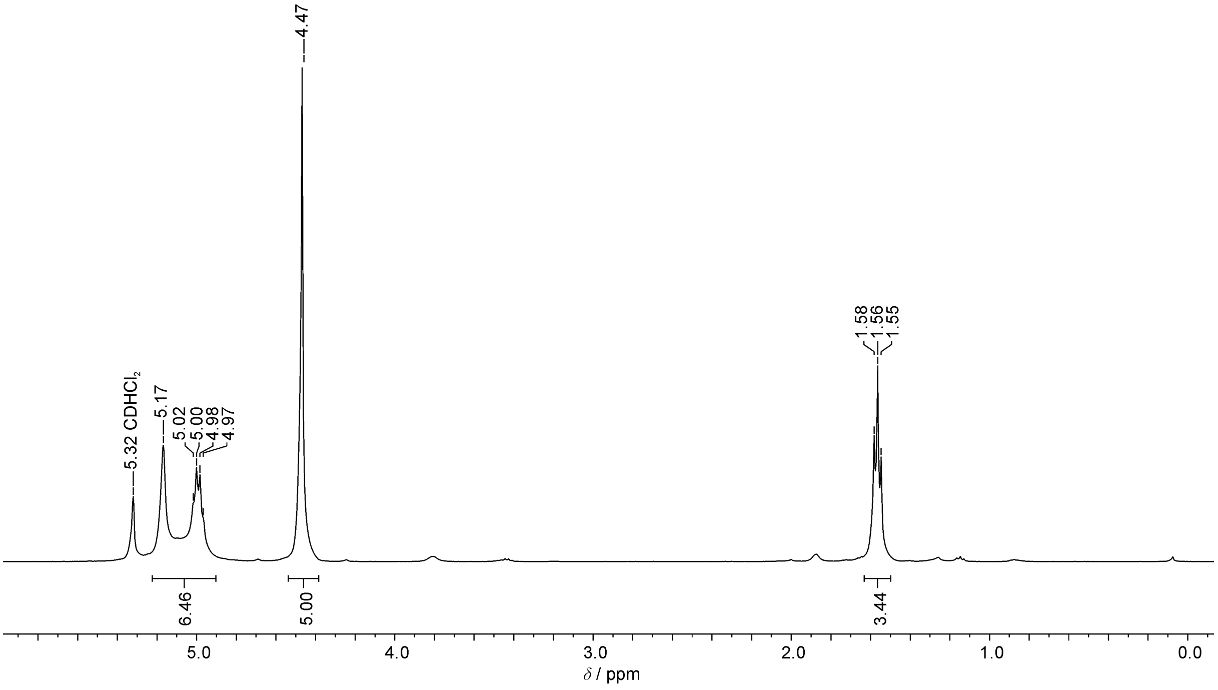

Fig. S02. ^{13}C{^{1}H} NMR spectrum of **1** in CD_2Cl_2.

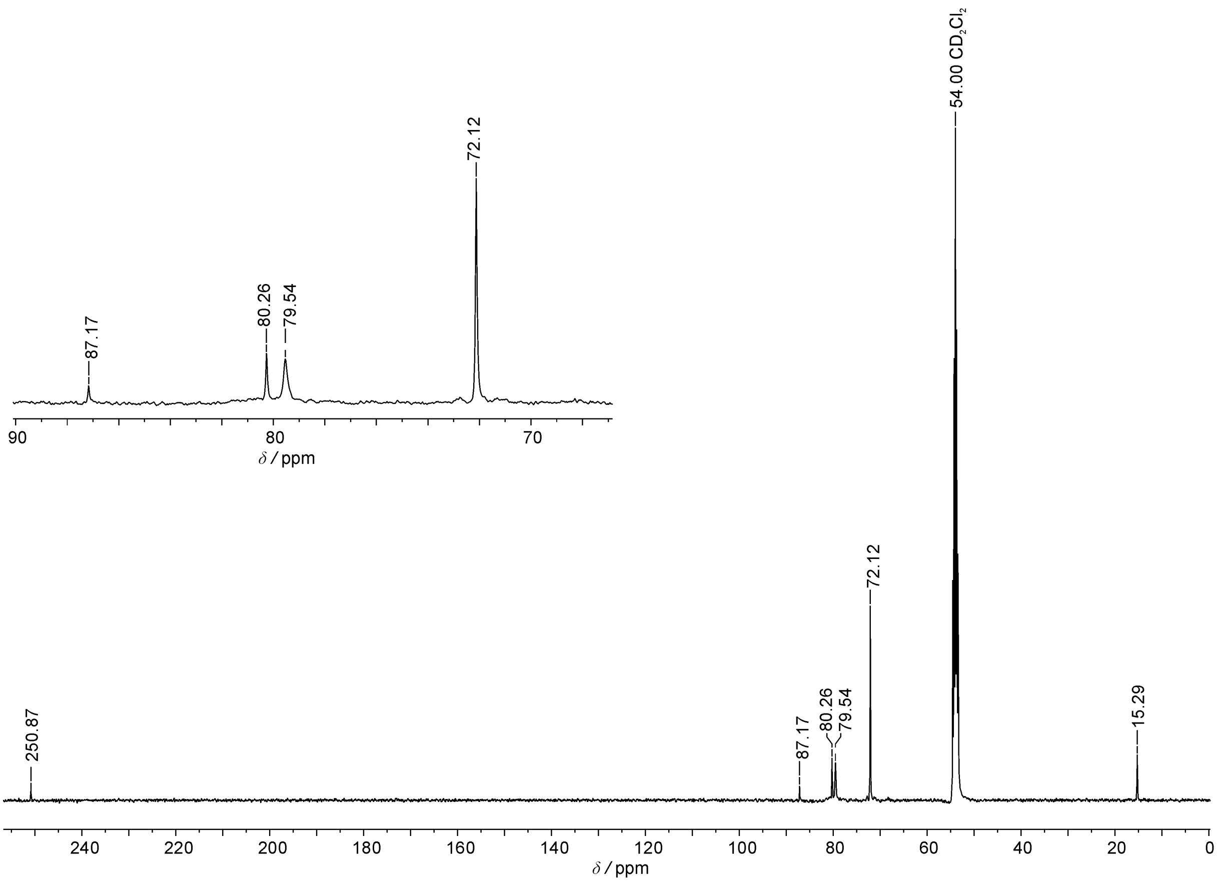

Fig. S03. ATR IR spectrum of **1**.

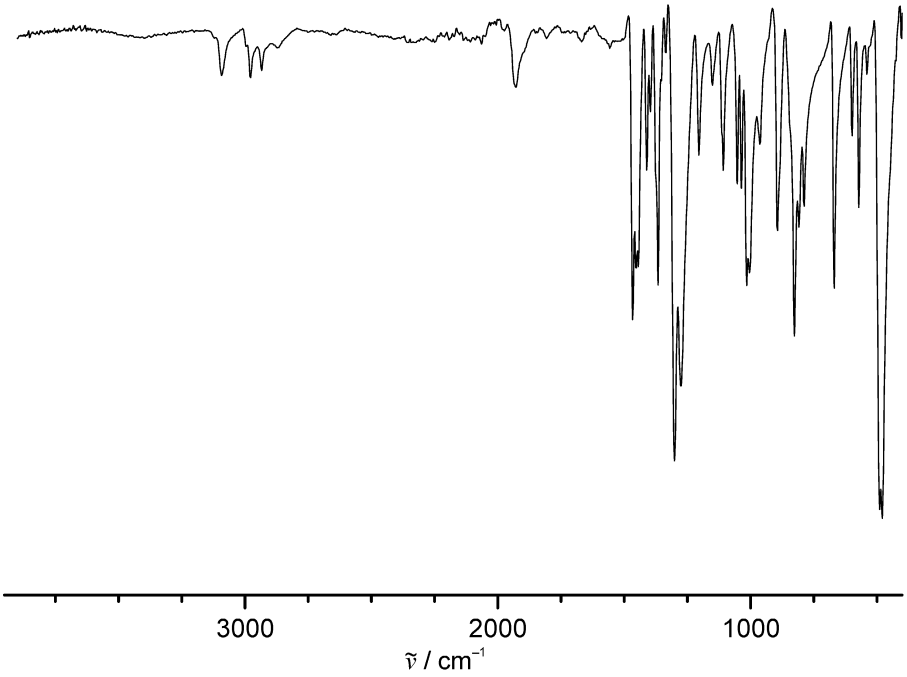

Fig. S04. UV/Vis absorption spectrum of **1** in CH_2Cl_2; oscillator strengths of DFT calculated transitions; difference electron densities (purple = depletion; orange = gain; contour value 0.01 a.u.) of the major transitions.

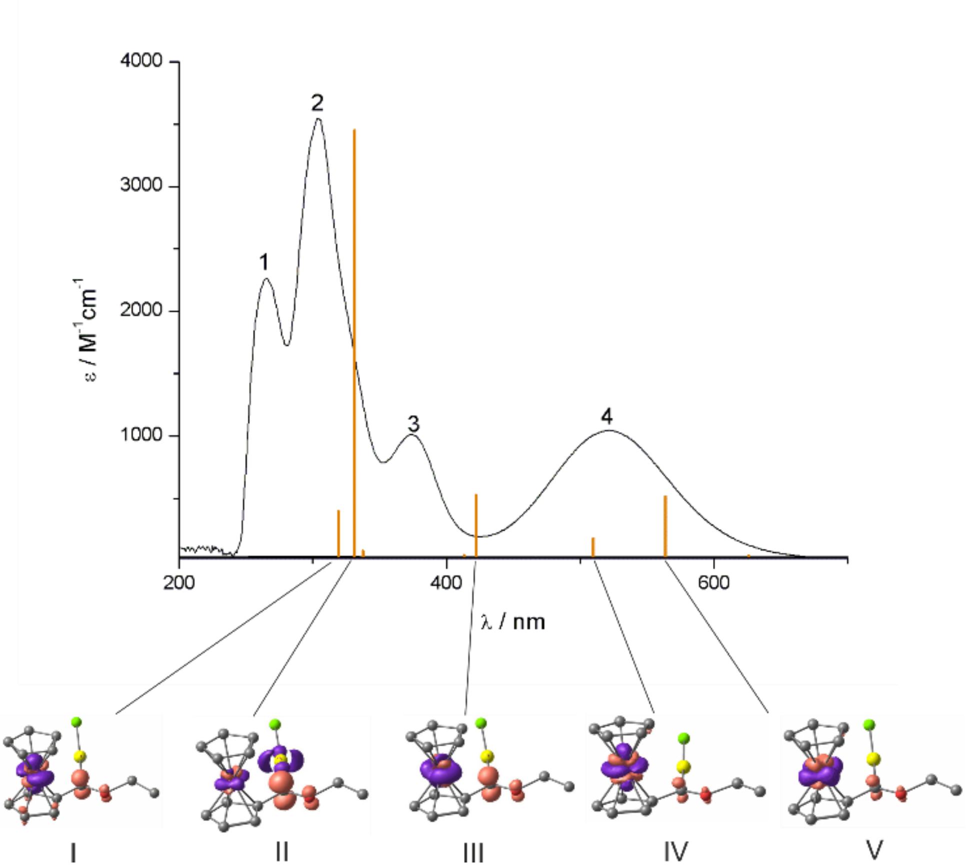

Fig. S05. LIFDI mass spectrum of **1** in CH_2Cl_2.

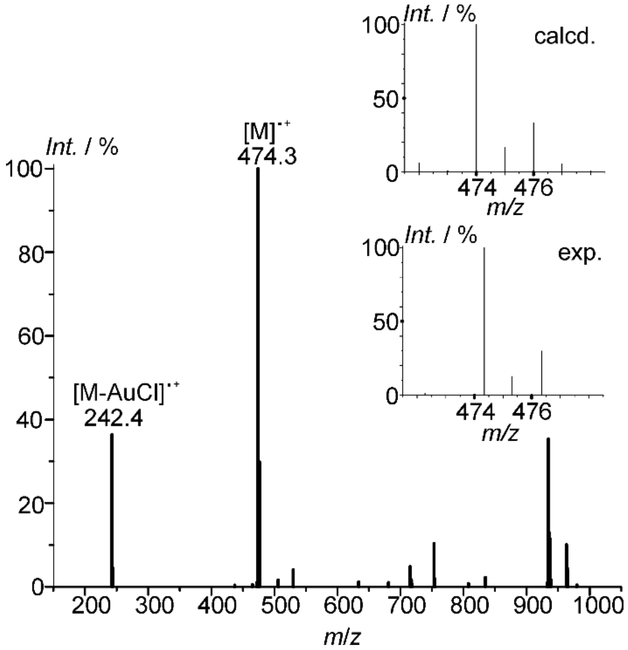

Fig. S06. Cyclic voltammogram of **1** in CH_2Cl_2 / [$^nBu_4N$][PF_6].

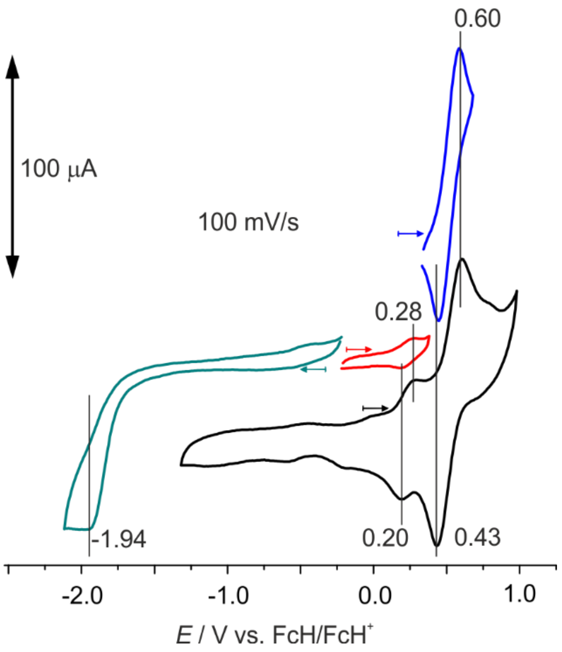

Fig. S07. Cyclic voltammogram of **1** in CH_2Cl_2 / [$^nBu_4N$][BAr^F_4].

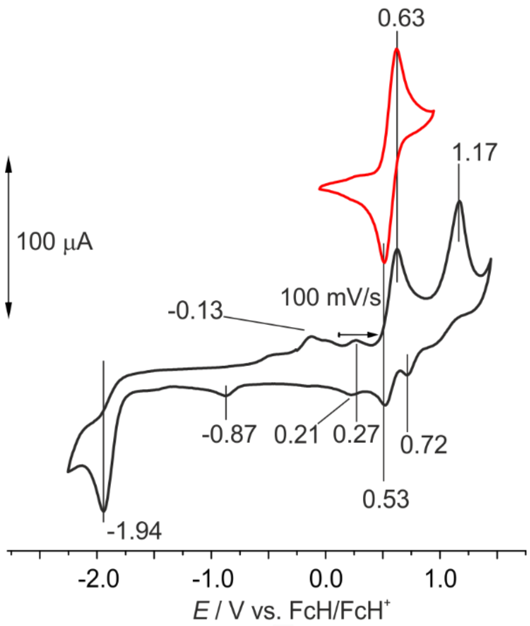

Fig. S08. Cyclic voltammogram of **1** in THF / $[^{n}\mathrm{Bu}_4\mathrm{N}][\mathrm{PF}_6]$.

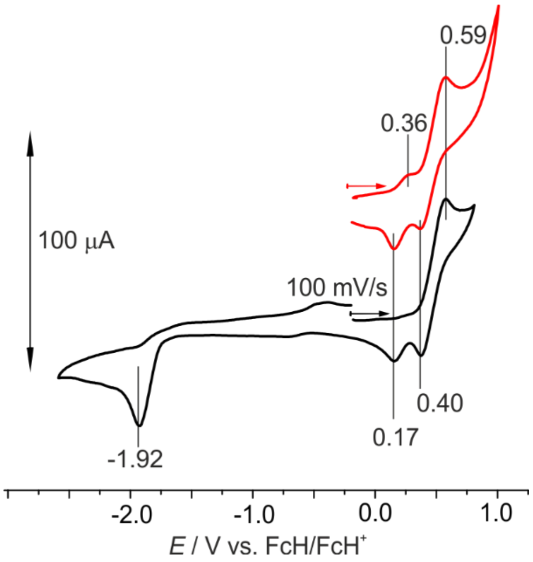

Fig. S9. Cyclic voltammogram of **1** in $\mathrm{CH_2Cl_2}$ / $[^{n}\mathrm{Bu}_4\mathrm{N}][\mathrm{BAr^F}_4]$.

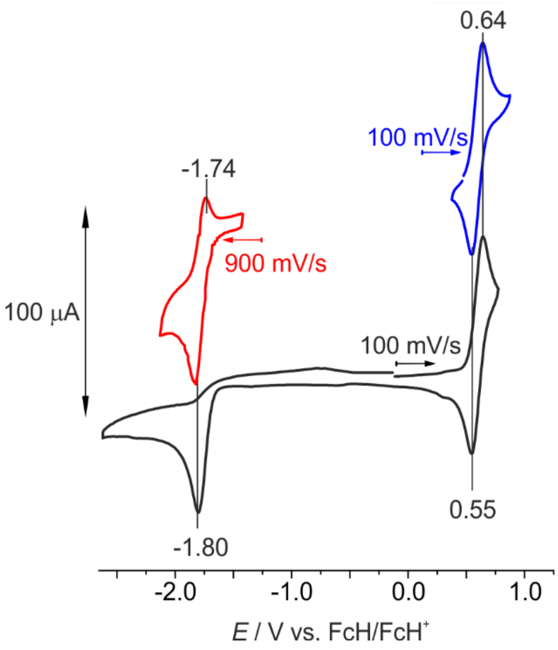

Fig. S10. ^{1}H DOSY of a mixture of **1** and W(CO)$_5$[C(Fc)OEt] in CD$_2$Cl$_2$ at 298 K; diffusion values in m^2 s^{-1} obtained from the respective sufficiently different Cp resonances (H^1).

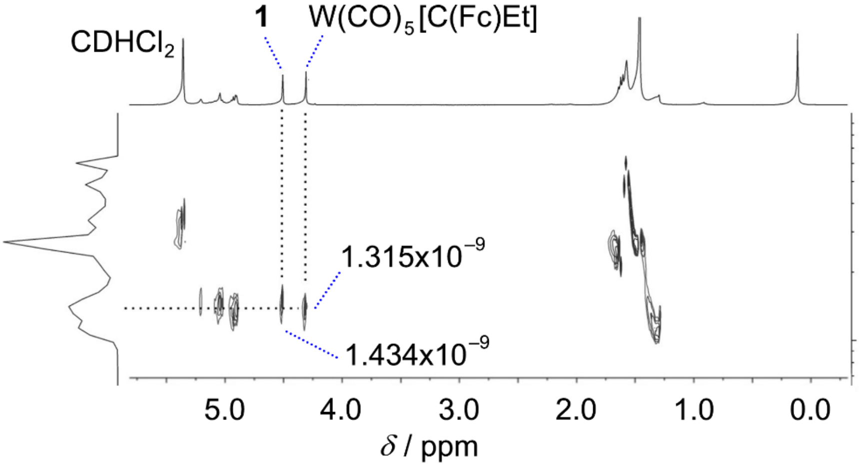

Fig. S11. X-band EPR spectrum of **1** (1.67 mᴍ) and Magic Blue (0.95 eq) in THF after 162 h at 77 K.

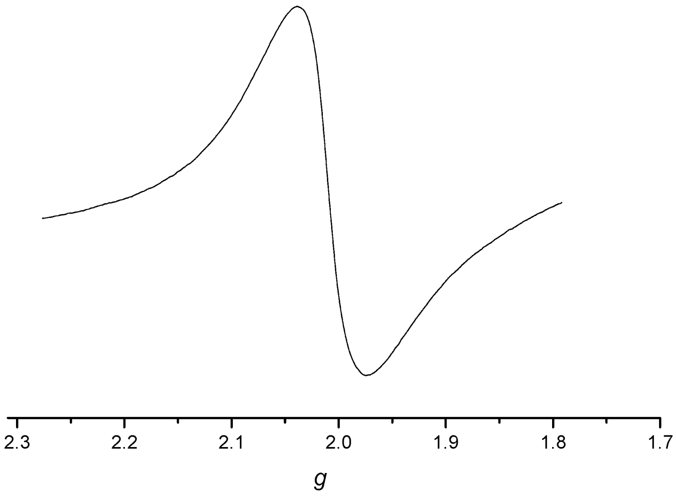

Fig. S12. X-band EPR spectrum of **1** (1.67 mᴍ) and Magic Blue (0.95 eq) in THF after 160 h at 298 K.

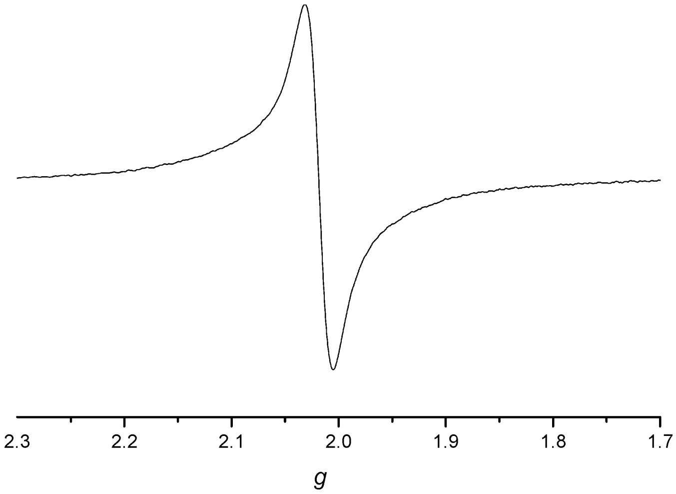

Fig. S13. X-band EPR spectrum of **1** (1.67 mM) and Magic Blue (0.95 eq) in CH_2Cl_2 (and 1 eq DMF as stabilizer) after 16 h at 77 K.

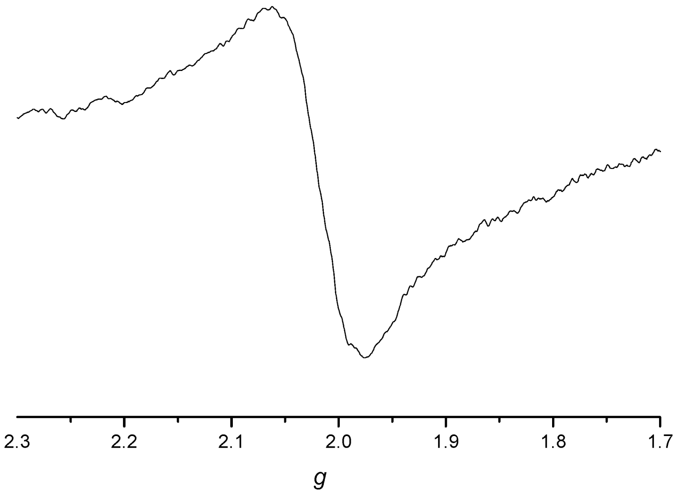

Fig. S14. X-band EPR spectrum of **1** (1.67 mM) and CAN (0.95 eq) in THF after 2 h at 77 K.

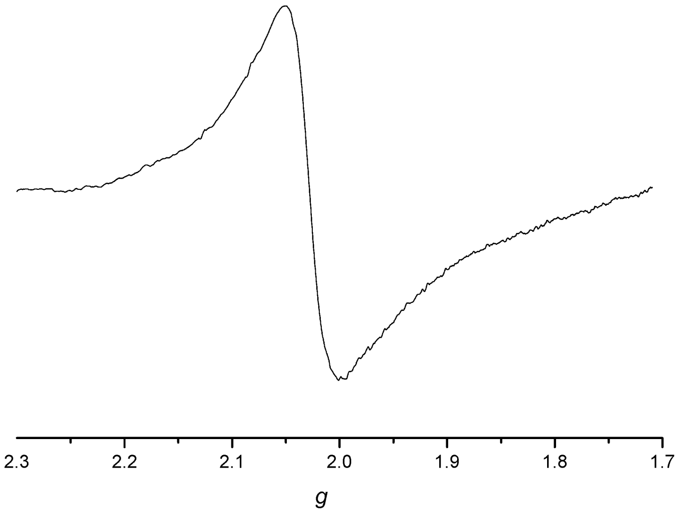

Fig. S15. X-band EPR spectrum of **1** (0.5 mM) and CAN (0.95 eq) in THF after 2.5 h at 298 K.

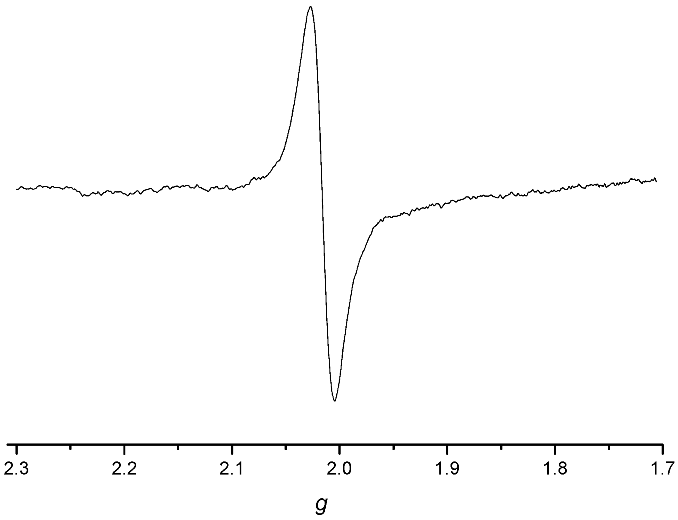

Fig. S16. X-band EPR spectrum of Magic Blue (5 mM) in THF at 298 K.

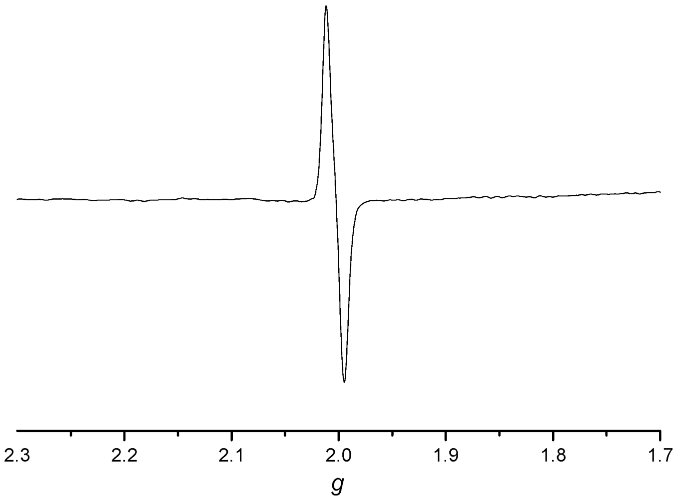

Fig. S17. X-band EPR spectra of Cu(TPP) in THF at different concentrations.

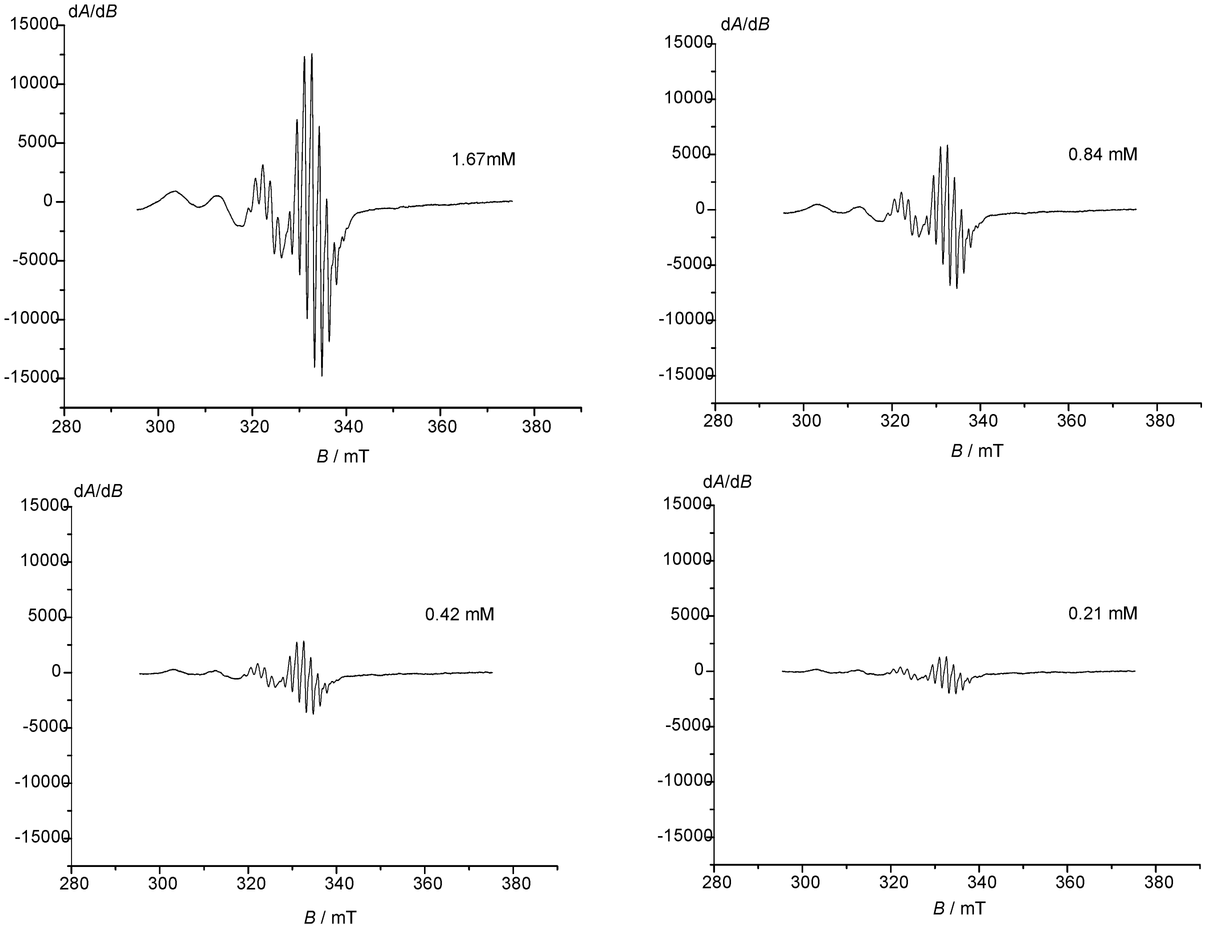

Fig. S18. Linear regression of the double integral of the EPR resonances of CuTPP versus concentration.

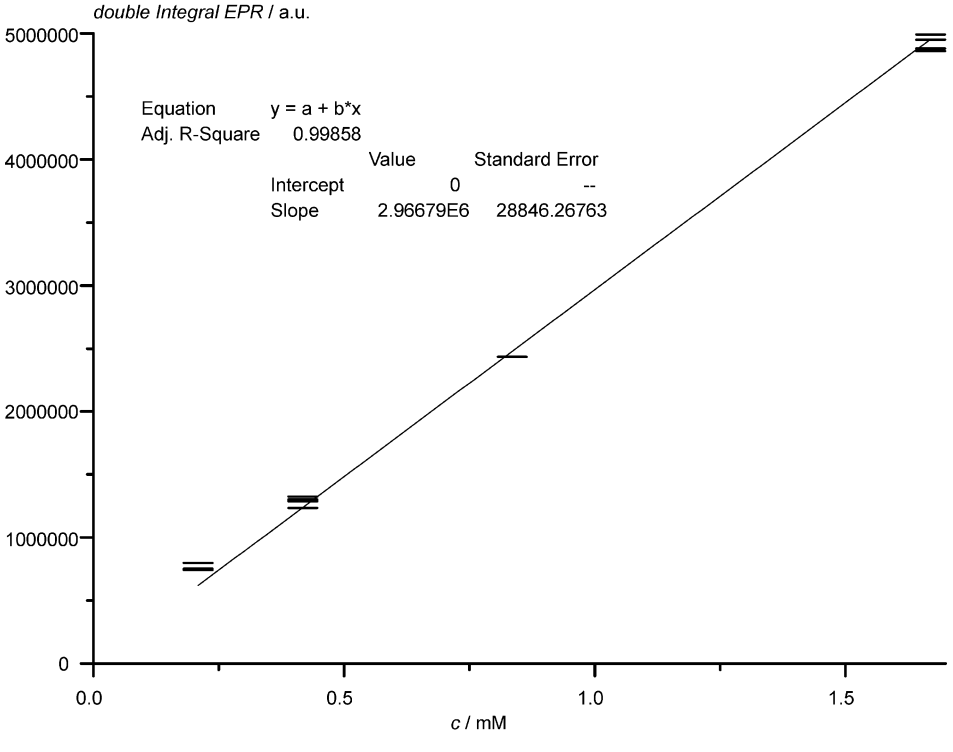

Equation y = a + b*x
Adj. R-Square 0.99858

	Value	Standard Error
Intercept	0	--
Slope	2.96679E6	28846.26763

Fig. S19. Conversion versus time plot for the catalytic reaction using **1** (1 mol-%) and Magic Blue (1.25 eq) in CD_2Cl_2. The determined TOF = $(8.3\pm1.1)\times10^{-3}$ s^{-1} is based on the conversion versus time plot without the induction period (ca. 2 h – 5 h).

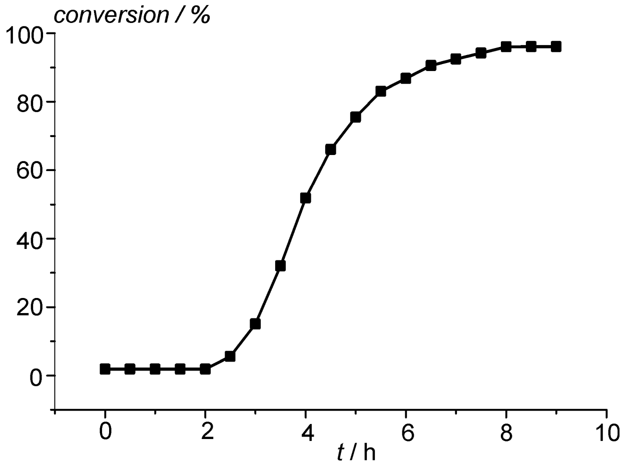

Fig. S20. Conversion versus time plots for the attempted reactions using **1** (1 mol-%) or Magic Blue (1 mol-%) alone in CD_2Cl_2.

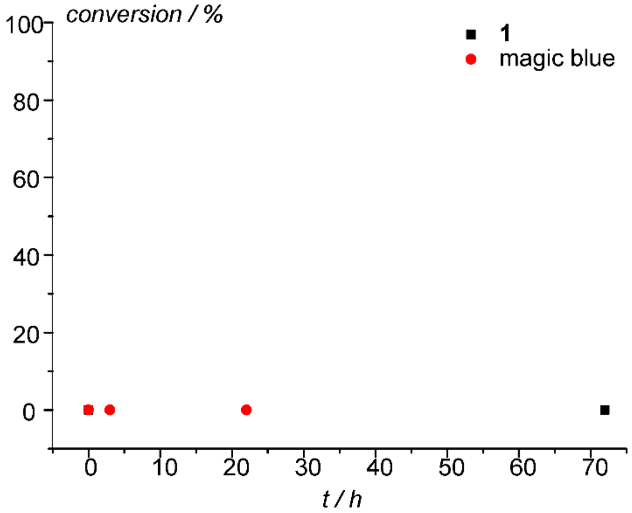

Fig. S21. ^{1}H NMR spectra of **1** and Magic Blue (1.0 eq) in CD_2Cl_2 over time.

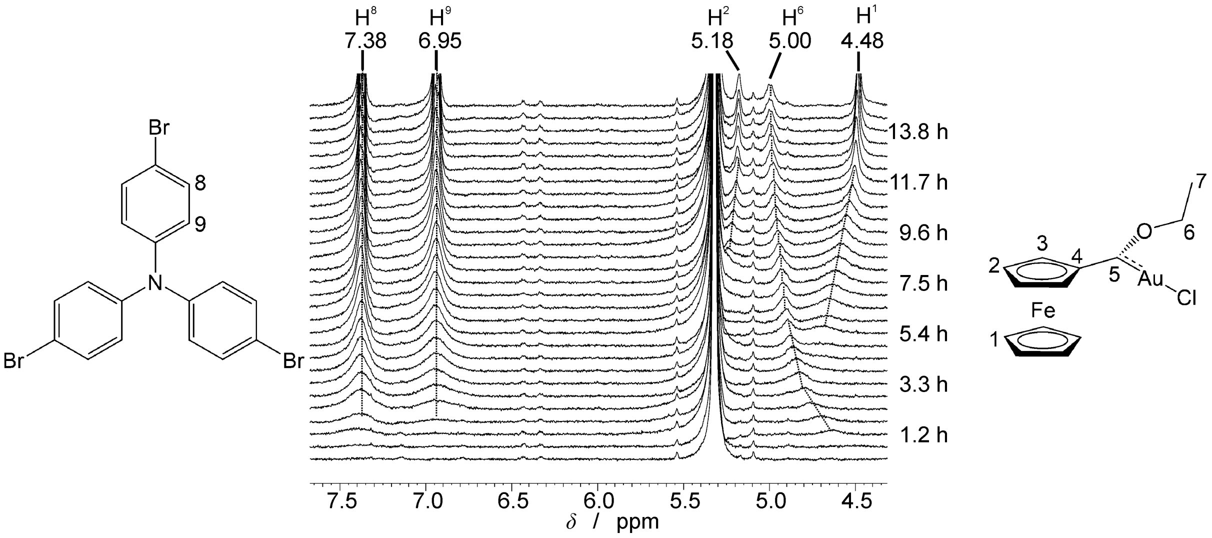

Fig. S22. ^{57}Fe Mößbauer spectrum of **1** and Magic Blue (0.95 eq) after 0.5 h in CH_2Cl_2 and removal the solvent by evaporation (Fc: $\delta = 0.520$ mm s^{-1}; $\Delta E_Q = 2.107$ mm s^{-1}; Fc$^+$: $\delta = 0.457$ mm s^{-1}; $\Delta E_Q = 0.243$ mm s^{-1}).

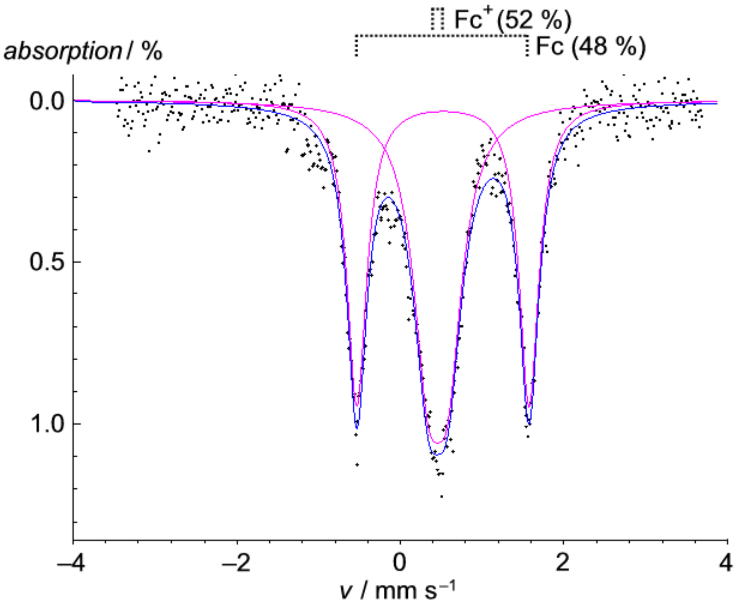

Fig. S23. ^{57}Fe Mößbauer spectrum of **1** and Magic Blue (0.95 eq) after 5 h in CH_2Cl_2 and removal of the solvent by evaporation (Fc: $\delta = 0.525$ mm s^{-1}; $\Delta E_Q = 2.291$ mm s^{-1}; Fc$^+$: $\delta = 0.47$ mm s^{-1}; $\Delta E_Q = 0.240$ mm s^{-1}; Fe^{II}: $\delta = 1.311$ mm s^{-1}; $\Delta E_Q = 2.650$ mm s^{-1}.

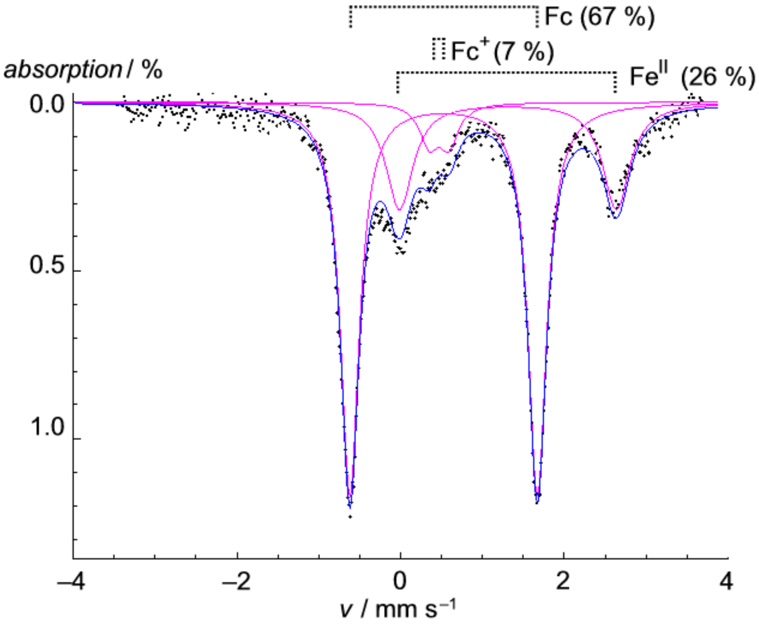

Fig. S24. Au L_3-edge XANES spectrum of **1**.

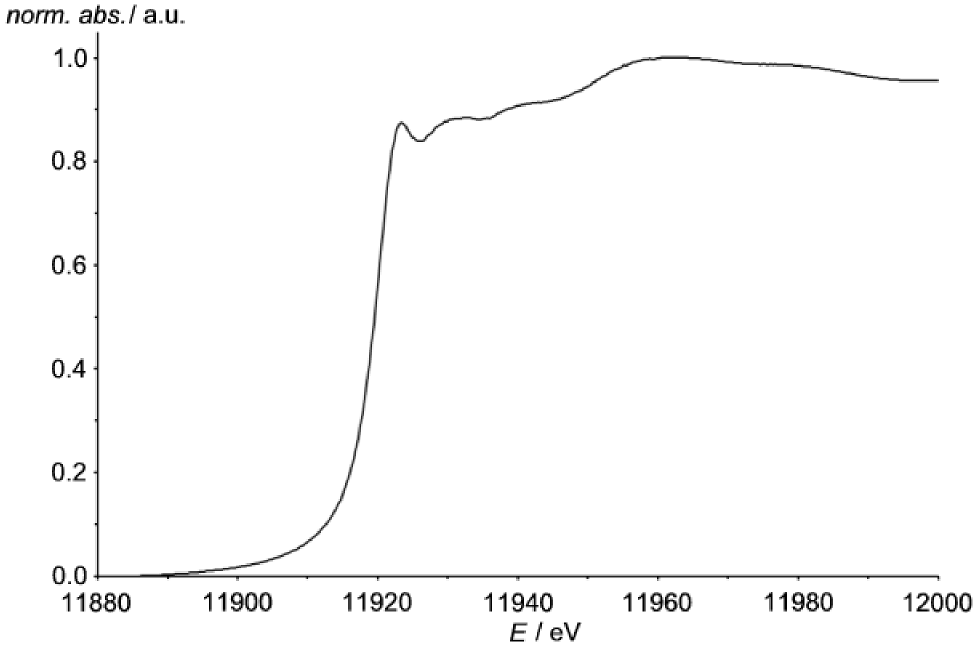

Fig. S25. Au L_3-edge XANES spectrum of **1** and Magic Blue (1.25 eq) after 5 h in CH_2Cl_2 and removal of the solvent (blue) and the spectrum of gold foil (red) for comparison.

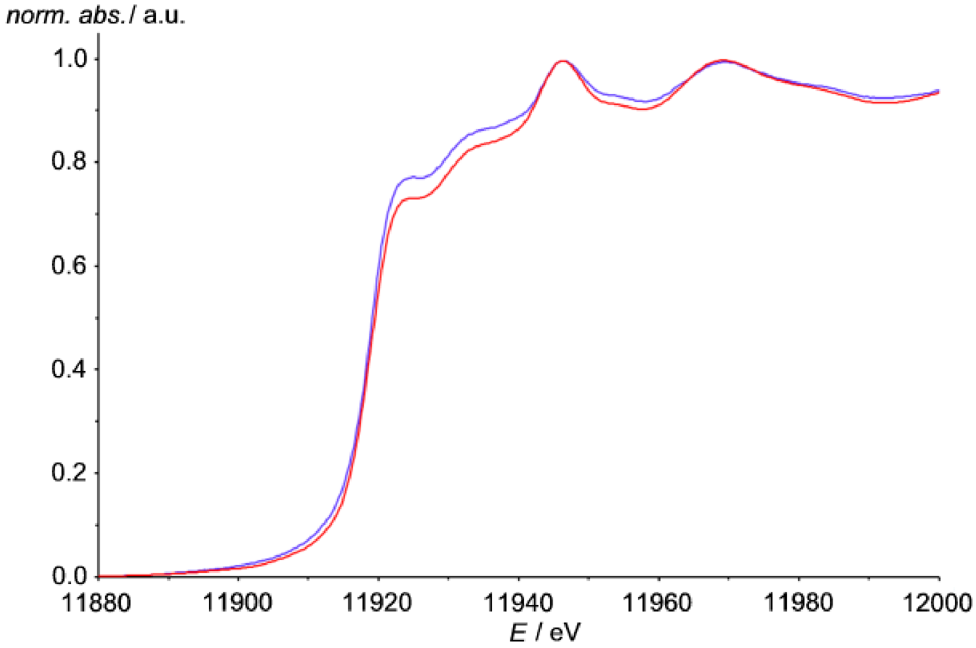

Fig. S26. Photographs of **1** in CH_2Cl_2 (left) and of the mixture of **1** and Magic Blue (1.0 eq) plus DMF (1 eq) after 14 h in CD_2Cl_2 (right) showing the precipitate.

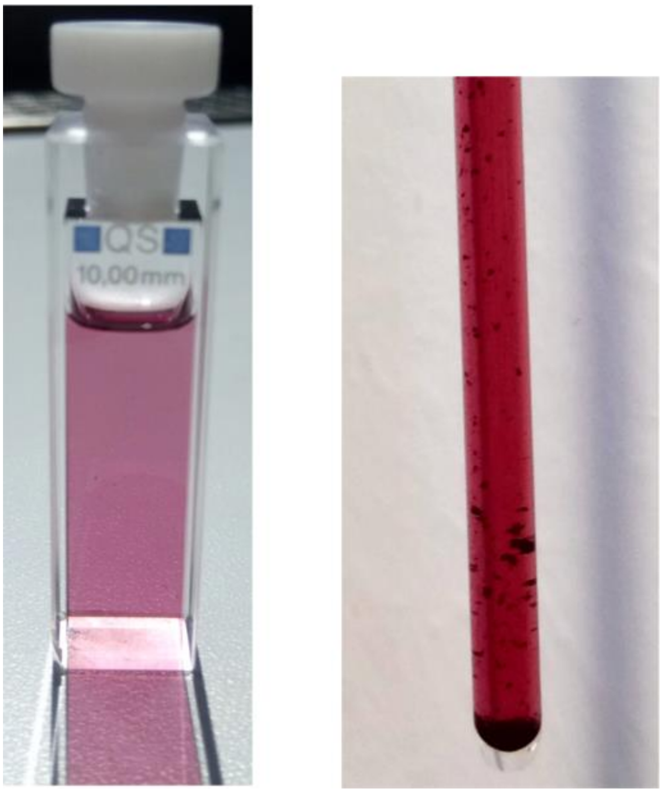

Fig. S27. Conversion versus time plot for the catalytic reaction using **1** (1 mol-%) and Magic Blue (1.25 eq) in CD_2Cl_2; second batch of substrate added.

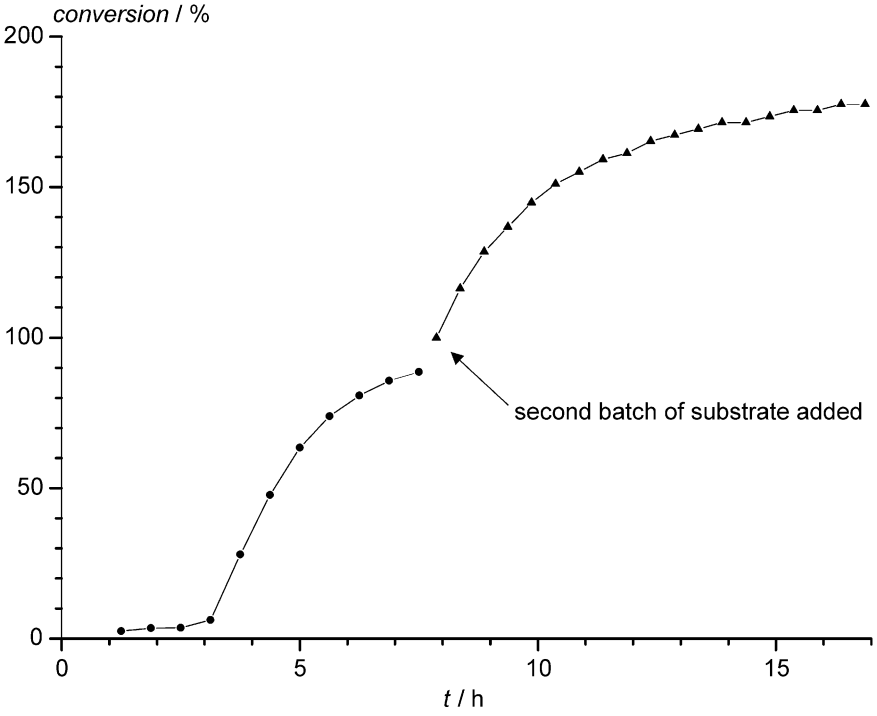

Fig. S28. Conversion versus time plot for the catalytic reaction using **1** (1 mol-%) and Magic Blue (1.25 eq) in the presence of [^{n}Bu$_4$N]Cl (42 eq) in CD_2Cl_2.

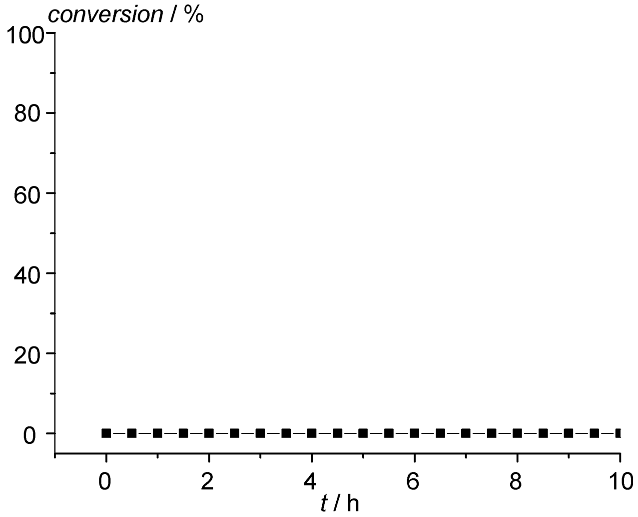

Fig. S29. Conversion versus time plot for the catalytic reaction using **1** (1 mol-%) and $AgSbF_6$ (1.25 eq) in CD_2Cl_2. The determined TOF = 3.2×10^{-3} s^{-1} is based on the conversion versus time plot (ca. 0 h – 5 h).

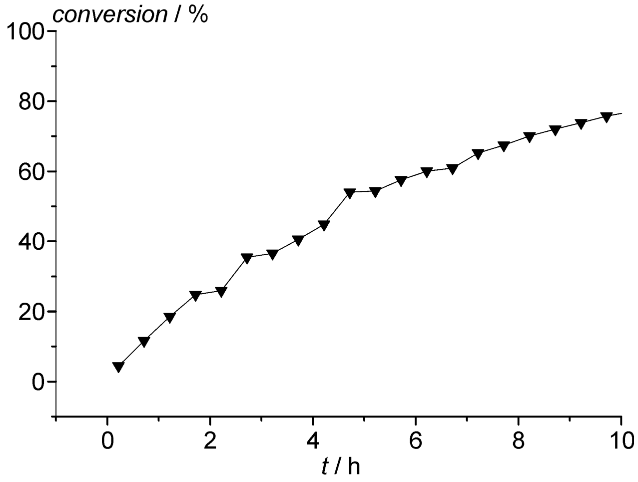

Fig. S30. ^{1}H NMR spectrum of **1** (0.01 mM; 10 mol-%) and Magic Blue (1.0 eq) at the beginning of the catalytic reaction and after ca. 63 % conversion stopped by addition of FeCp*$_2$ (1.05 eq) indicating a 84±5 % recovery.

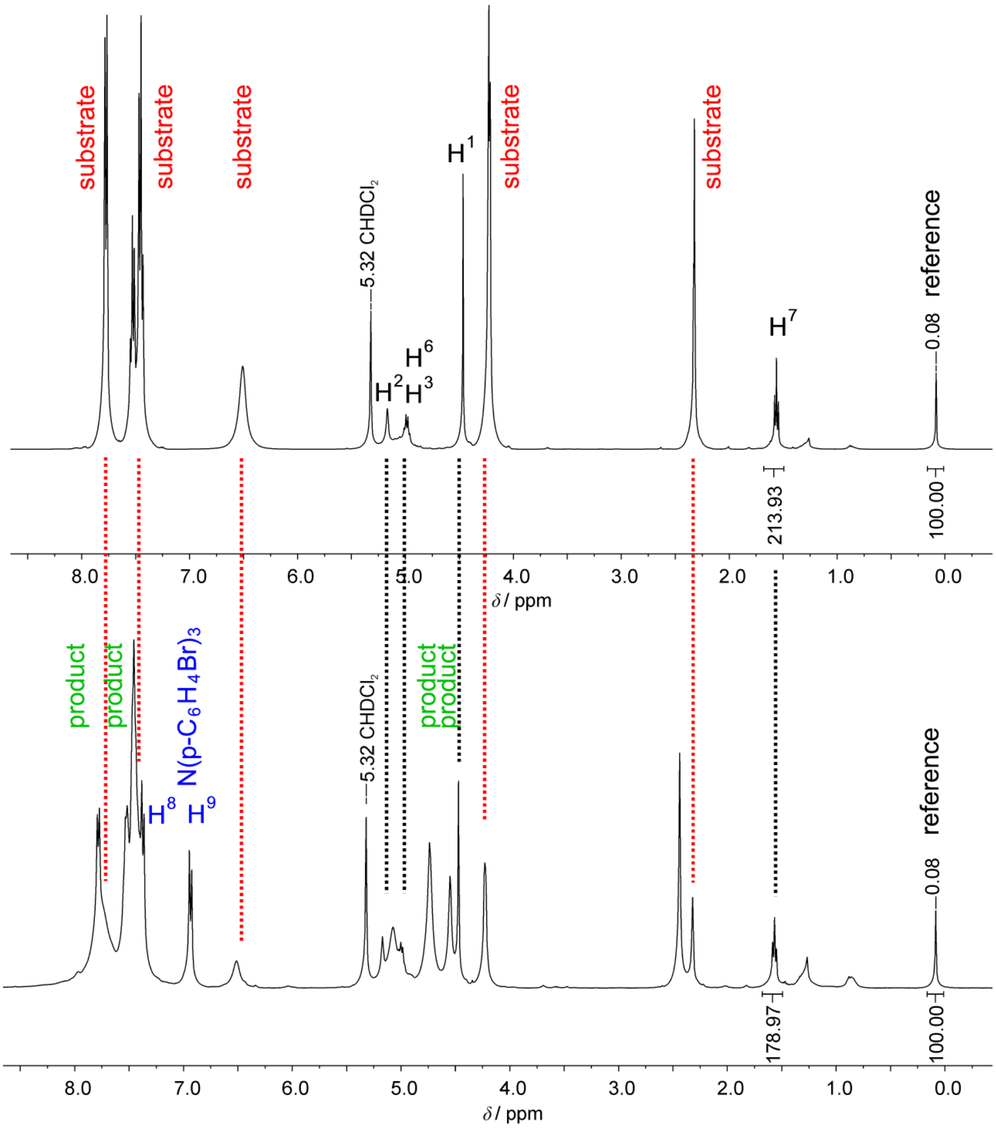

Cartesian coordinates of optimised geometries (CPCM(CH_2Cl_2)-B3LYP-D3(BJ)-ZORA/def2-TZVP)

1

6	6.467719000	2.708355000	7.408761000
79	6.488827000	1.432731000	5.884878000
6	7.463616000	2.675259000	8.432471000
6	7.370792000	3.265546000	9.747948000
1	6.611435000	3.955156000	10.074072000
6	8.429758000	2.747635000	10.524156000
1	8.615623000	2.968355000	11.562731000
6	9.182506000	1.838333000	9.722172000
1	10.031700000	1.263247000	10.053046000
6	8.593355000	1.774667000	8.442433000
1	8.913555000	1.166713000	7.613129000
26	7.193551000	1.216670000	9.824115000
6	6.501245000	0.211422000	11.484775000
1	6.765386000	0.461689000	12.499299000
6	5.404017000	0.745088000	10.748385000
1	4.690918000	1.469767000	11.105701000
6	5.440041000	0.180856000	9.443677000
1	4.765803000	0.411903000	8.635213000
6	7.212430000	-0.679424000	10.631809000
6	6.559942000	-0.694958000	9.366309000
1	6.872684000	-1.246098000	8.494778000
1	8.111198000	-1.216613000	10.887683000
8	5.541565000	3.597621000	7.627200000
6	4.401987000	3.702496000	6.717123000
1	4.793964000	3.953857000	5.732296000
1	3.925482000	2.724038000	6.675454000
6	3.480927000	4.763809000	7.260681000
1	3.984038000	5.730210000	7.311763000
1	3.121773000	4.496544000	8.255375000
1	2.619814000	4.857959000	6.597092000
17	6.528771000	-0.148655000	4.176376000

[1][SbCl$_6$] Au^{I}Fe^{III} isomer

6	6.104522000	2.896333000	7.608091000
79	6.167687000	2.172817000	5.774038000
6	7.250724000	3.526242000	8.243443000
6	7.388378000	3.874682000	9.634820000
1	6.635720000	3.749990000	10.394835000
6	8.693190000	4.378922000	9.819870000
1	9.124163000	4.681850000	10.760711000
6	9.371654000	4.348915000	8.573590000
1	10.400438000	4.624071000	8.411854000
6	8.502359000	3.820138000	7.598705000
1	8.737714000	3.639934000	6.562563000
26	8.701433000	2.346467000	9.076491000
6	9.763268000	1.075907000	10.396929000
1	10.271085000	1.434290000	11.277847000
6	8.390694000	0.710405000	10.313422000
1	7.680794000	0.717837000	11.124071000
6	8.116794000	0.366134000	8.955779000
1	7.164720000	0.058360000	8.555181000
6	10.332994000	0.954240000	9.103949000
6	9.322662000	0.522596000	8.212349000
1	9.436968000	0.388221000	7.149983000
1	11.339201000	1.220917000	8.825782000
8	5.092864000	2.851756000	8.403393000
6	3.832934000	2.217092000	7.973128000
1	3.546947000	2.687568000	7.034535000
1	4.057551000	1.165755000	7.802807000
6	2.823745000	2.428537000	9.068516000
1	2.636289000	3.490686000	9.228726000
1	3.159461000	1.977594000	10.002886000
1	1.886694000	1.953346000	8.774373000
17	6.224686000	1.310715000	3.632100000
17	9.694503000	1.705092000	4.711933000
51	12.122516000	1.710579000	4.703175000
17	14.544540000	1.720909000	4.716545000
17	12.120510000	0.331768000	2.712896000
17	12.125458000	3.086318000	6.721621000
17	12.129295000	-0.287236000	6.096067000
17	12.108781000	3.720823000	3.347062000

[1][SbCl$_6$] Au^{II}Fe^{II} isomer

6	6.219418000	2.465011000	7.575240000
79	5.672987000	1.106229000	6.175824000
6	6.060196000	3.847594000	7.335763000
6	6.509513000	4.915315000	8.204206000
1	6.882572000	4.793841000	9.206409000
6	6.365870000	6.122851000	7.493457000
1	6.638805000	7.100326000	7.856611000
6	5.863810000	5.834310000	6.189441000
1	5.694298000	6.556891000	5.408348000
6	5.689111000	4.443195000	6.070317000
1	5.333541000	3.910506000	5.204658000
26	7.662022000	4.812551000	6.508921000
6	9.588914000	5.486356000	6.838332000
1	9.855129000	6.147012000	7.647405000
6	9.546792000	4.067930000	6.897925000
1	9.793331000	3.460923000	7.753820000
6	9.086556000	3.590848000	5.633109000
1	8.918266000	2.562491000	5.367036000
6	9.142660000	5.886896000	5.547588000
6	8.839261000	4.712273000	4.802082000
1	8.446328000	4.682627000	3.799283000
1	9.022307000	6.902308000	5.207045000
8	6.622786000	2.139032000	8.754588000
6	6.955813000	0.761266000	9.126920000
1	6.474811000	0.620623000	10.091650000
1	6.505940000	0.091684000	8.394484000
6	8.454861000	0.623698000	9.204006000
1	8.872963000	1.323897000	9.927343000
1	8.916725000	0.797882000	8.231550000
1	8.697935000	-0.391326000	9.522008000
17	3.272142000	1.487063000	6.605686000
17	5.205393000	-0.520945000	4.379330000
51	7.497331000	-0.457235000	3.257992000
17	9.689720000	-0.314655000	2.351642000
17	7.145122000	1.920449000	3.038549000
17	7.674972000	-2.809369000	3.674790000
17	6.430860000	-0.853391000	1.156051000
17	8.350824000	-0.056445000	5.538056000

[**1**+substrate]$^+$ Au^{I}Fe^{III} isomer

6	0.089265000	0.167235000	1.224885000
79	0.721916000	-1.172480000	-0.082884000
8	-0.059001000	0.004156000	2.489607000
6	0.338033000	-1.264710000	3.122171000
1	-0.125426000	-2.066879000	2.550564000
1	1.419117000	-1.323170000	3.022751000
17	1.451106000	-2.681852000	-1.681058000
8	2.955134000	0.880234000	2.005989000
6	3.459258000	0.606215000	0.915500000
7	4.260611000	-0.463197000	0.734119000
6	4.546856000	-1.415517000	1.794422000
6	3.655206000	-2.575029000	1.779492000
6	2.912392000	-3.516486000	1.744932000
1	4.653152000	-0.639270000	-0.175748000
1	5.581466000	-1.744588000	1.691279000
1	4.456232000	-0.893890000	2.747294000
1	2.245768000	-4.344986000	1.701936000
6	-0.321248000	1.501288000	0.808045000
6	-0.178275000	2.032568000	-0.518652000
1	0.294813000	1.534412000	-1.347793000
6	-0.766721000	3.314890000	-0.532624000
1	-0.855814000	3.956493000	-1.394022000
6	-1.281383000	3.589700000	0.761089000
1	-1.838050000	4.469816000	1.041250000
6	-1.015722000	2.484483000	1.595025000
1	-1.305625000	2.377240000	2.626777000
26	-2.177211000	1.770143000	-0.012401000
6	-3.762207000	1.717509000	-1.430357000
1	-3.831495000	2.398505000	-2.263304000
1	-2.489670000	0.068676000	-2.233739000
6	-3.041821000	0.493020000	-1.411406000
6	-3.147960000	-0.054487000	-0.097867000
1	-2.701211000	-0.974752000	0.241284000
6	-3.932090000	0.841179000	0.687271000
1	-4.165382000	0.730087000	1.733731000
6	-4.309637000	1.929075000	-0.139785000
1	-4.859258000	2.801396000	0.175995000
6	3.216403000	1.456518000	-0.291866000
6	2.985348000	2.818969000	-0.102824000
6	3.163044000	0.921827000	-1.580404000
6	2.723447000	3.641597000	-1.189813000
6	2.877989000	1.742839000	-2.664847000
6	2.664197000	3.104084000	-2.472435000
1	3.010525000	3.221901000	0.900414000
1	3.298993000	-0.138739000	-1.743211000
1	2.553172000	4.699411000	-1.036019000
1	2.815702000	1.316811000	-3.657698000
1	2.445491000	3.743091000	-3.318433000
6	-0.122171000	-1.221837000	4.552927000
1	-1.207830000	-1.138335000	4.614532000
1	0.180353000	-2.148333000	5.043587000
1	0.333556000	-0.386373000	5.085165000

[**1**+substrate]$^+$ CPCM(CH_2Cl_2)-B3LYP-D3(BJ)-ZORA/def2-TZVP Au^{II}Fe^{II} isomer

6	-0.649170836	-0.389292947	1.109024278
79	0.224971770	-1.798617906	-0.083334833
8	-1.097323111	-0.633763311	2.288425955
6	-1.062780007	-1.999084006	2.844051483
1	-1.645717961	-2.627405259	2.173940045
17	-1.962065941	-2.856890381	-0.674917955
8	2.238153058	-0.656052786	1.081911882
6	3.087113177	-0.207765042	0.285870017
7	3.683460482	-1.026068336	-0.596306029
6	3.439181151	-2.453455172	-0.571691878
6	2.132267336	-2.840767409	-1.119473941
6	1.124832919	-3.269261278	-1.649666152
1	4.280839153	-0.660130097	-1.319147334
1	4.205867437	-2.944052224	-1.171922286
1	3.516816216	-2.824332222	0.450723018
1	0.362445140	-3.741880062	-2.229444917
1	-0.020569120	-2.315234074	2.838216245
6	-0.703633229	0.953256192	0.674984102
6	-0.352236781	1.414561167	-0.651083283
1	0.095512789	0.816579234	-1.427352969
6	-0.688069068	2.778615012	-0.730306938
1	-0.567423005	3.405488435	-1.598219011
6	-1.265340062	3.180389134	0.510911109
1	-1.652907892	4.161450415	0.731894999
6	-1.300003289	2.070566327	1.378568118
1	-1.683588001	2.045851104	2.383928161
26	-2.362760012	1.598887891	-0.309932235
6	-3.630335319	1.810209004	-1.921403961
1	-3.368234357	2.338105115	-2.823891417
1	-2.936968128	-0.279299223	-2.324949239
6	-3.397937076	0.431239770	-1.659753329
6	-3.850341290	0.157708050	-0.336339239
1	-3.768338396	-0.792059806	0.164951957
6	-4.352511449	1.362535106	0.221371248
1	-4.734882228	1.487997211	1.221086027
6	-4.213809329	2.387993300	-0.758495151
1	-4.474373561	3.425997229	-0.630734301
6	3.453371039	1.229144868	0.284488864
6	2.630878249	2.113173034	0.987236251
6	4.580182551	1.719680006	-0.382351200
6	2.920276291	3.468813489	1.010352301
6	4.869431365	3.076225355	-0.353584067
6	4.039312073	3.952791063	0.339695281
1	1.766107372	1.727947342	1.505456885
1	5.252625545	1.054405248	-0.907363824
1	2.273934436	4.147643123	1.551017988
1	5.745925635	3.449099520	-0.866893936
1	4.268724169	5.010455514	0.360488771
6	-1.640309240	-1.933954987	4.231108133
1	-2.673444209	-1.586341098	4.206448474
1	-1.623993118	-2.935897074	4.662591324
1	-1.053453258	-1.273329051	4.869850473